THE JOURNAL OF BIOLOGICAL CHEMISTRY VOL. 282, NO. 46, pp. 33776–33787, November 16, 2007

Amplitude Control of Protein Kinase C by RINCK, a Novel E3 Ubiquitin Ligase*

Received for publication, April 20, 2007, and in revised form, September 14, 2007 Published, JBC Papers in Press, September 24, 2007, DOI 10.1074/jbc.M703320200

Dan Chen[‡§1], **Christine Gould**[‡¶], **Renee Garza**[‖], **Tianyan Gao**[‡2], **Randolph Y. Hampton**[‖], **and Alexandra C. Newton**[‡3]

From the [‡]*Department of Pharmacology,* [§]*Molecular Pathology Graduate Program,* [¶]*Biomedical Sciences Graduate Program,* [‖]*Division of Biology, University of California at San Diego, La Jolla, California 92093-0721*

Protein kinase C (PKC) isozymes play a central role in cellular signaling. Levels of PKC control the amplitude of agonist-induced signaling and alterations in these levels are associated with disease states, most notably cancer, yet mechanisms that control the turnover of the protein are poorly understood. Here we identify an E3 ligase that catalyzes the ubiquitin-mediated degradation of PKC. Specifically, we identified a RING finger domain-containing protein, RINCK (for RING-finger protein that interacts with C kinase) from a yeast two-hybrid screen using the amino terminus of PKCβ as bait. RINCK encodes a protein of 581 amino acids that contains a RING finger domain, a B-box, and two coiled-coil regions, the three domains that form the signature motif of the large family of diverse TRIM (tripartite motif) proteins. Co-immunoprecipitation studies using tsA201 cells reveal that RINCK and PKC associate with each other in cells. Studies using fragments of PKCβ reveal that this interaction is mediated by the C1A domain of PKC. RINCK induces the ubiquitination of PKC both *in vitro* and in cells. Overexpression of RINCK reduces the levels of PKC in cells, whereas genetic knockdown of endogenous RINCK increases the levels of PKC. This increase was observed for all PKC isozymes examined (including conventional, novel, and atypical). The RINCK-mediated degradation of PKC occurs independently of the classic phorbol ester-mediated down-regulation: genetic depletion of RINCK had no effect on the phorbol ester-mediated down-regulation and, additionally, up-regulated the levels of isozymes that cannot bind phorbol esters. Our data reveal a novel mechanism that provides amplitude control in PKC signaling through ubiquitination catalyzed by RINCK, an E3 ligase that specifically recognizes the C1 domain of PKC isoforms.

The signaling lifetime of protein kinase C (PKC)[4] is under the control of multiple mechanisms. Phosphorylation controls the stability of PKC, thus setting the signaling amplitude in pathways controlled by PKC. Binding of lipid second messengers to its regulatory domains reversibly controls the acute propagation of PKC signals, thus setting the gain (1). Chronic activation of PKC, as occurs with phorbol esters, results in its ultimate degradation, a process referred to as "down-regulation" (2). Despite extensive studies characterizing both the phorbol ester-mediated down-regulation of PKC and the effect of phosphorylation on protein stability, the molecular mechanisms controlling the degradation of PKC are poorly understood. PKC levels are altered in a variety of diseased states, most notably cancer (3–7), underscoring the importance of understanding how the lifetime of the protein is controlled.

The ubiquitin-proteasome pathway plays a major role in controlling protein degradation in the cell and mounting evidence points to a key role in controlling the lifetime of signaling molecules such as protein kinases (8). Conjugation of ubiquitin, a 76-residue polypeptide, on Lys residues of target proteins proceeds via three sequential steps: activation of ubiquitin by an activating enzyme E1, transfer of ubiquitin to a conjugating enzyme E2, and transfer of ubiquitin to the substrate facilitated by the ubiquitin ligase E3 (9, 10). Specificity is dictated by the E3 ligase, which recognizes specific determinants on both the substrate and the E2 enzyme (11). E3s fall into two major classes, those containing a HECT domain and those containing a RING domain. HECT domain E3 ligases participate in the catalytic step by forming a thioester intermediate during ubiquitin transfer, whereas RING E3 ligases serve as a scaffold to bring together the substrate and the E2 and do not participate in the catalytic step. The RING domain is an ~70-residue globular domain with defined spacing of Cys and His residues to coordinate two zinc ions that maintain the fold of the domain (9); this module binds E2.

PKC comprises a family of 10 isozymes, grouped into conventional (α, γ, and two C-terminal splice variants, βI and βII), novel (δ, ϵ, η, θ), and atypical (ζ, ι/λ) isozymes based on their cofactor dependence. All isozymes contain a C1 domain, a membrane-targeting module that binds phosphatidylserine and, in the case of all but the atypical isozymes, binds diacylglycerol/phorbol esters. Novel PKCs and conventional PKCs also contain a C2 domain; this domain serves as a Ca^{2+}-regulated membrane-targeting module in conventional PKC

* This work was supported by National Institutes of Health Grant P01 DK54441 (to A. C. N.). The costs of publication of this article were defrayed in part by the payment of page charges. This article must therefore be hereby marked "*advertisement*" in accordance with 18 U.S.C. Section 1734 solely to indicate this fact.

[1] Present address: Dept. of Genetics, Harvard Medical School, 77 Ave. Louis Pasteur, Boston, MA 02115.

[2] Present address: Dept. of Pharmacology and Toxicology, University of Texas Medical Branch, 301 University Blvd., Galveston, TX 77555-1048.

[3] To whom correspondence should be addressed: 9500 Gilman Dr., La Jolla, CA 92093-0721. Tel.: 858-534-4527; Fax: 858-822-5888; E-mail: anewton@ucsd.edu.

[4] The abbreviations used are: PKC, protein kinase C; GST, glutathione *S*-transferase; HECT, homologous to E6-associated protein (E6AP) COOH terminus; PDBu, 4β-phorbol 12,13-dibutyrate; PKA, protein kinase A; RINCK, RING finger protein that interacts with C kinase; RING, really interesting new gene; TRIM, tripartite motif; HA, hemagglutinin; PP1, protein phosphatase 1; siRNA, small interfering RNA.

isozymes. PKC isozymes are processed by a series of ordered phosphorylations that converts all family members into mature, stable species. Impairment of this processing results in rapid degradation of PKC by an as yet unidentified quality control pathway. For example, PKC isozymes are depleted in cells lacking the upstream kinase that initiates the ordered phosphorylations, the phosphoinositide-dependent kinase PDK-1 (12). In addition to unprocessed PKC, the ligand-activated form of PKC is highly sensitive to dephosphorylation and degradation (13). Most notably, constitutive activation of PKC by phorbol esters leads to the eventual down-regulation of phorbol ester-sensitive PKCs by a process that requires the intrinsic activity of PKC (14, 15). Nonetheless, the mechanism of this down-regulation remains to be elucidated. Several studies indicate that PKC isozymes become ubiquitinated following activation. PKC α, δ, and ϵ have been reported to become ubiquitinated following treatment of cells with phorbol esters or another potent PKC agonist, bryostatin (16–19). Both proteasome-sensitive and -insensitive pathways have been proposed to regulate PKC degradation (18, 20). The specific machinery controlling the degradation of unprocessed or activated PKC remains to be elucidated.

In this report we identify a novel RING domain E3 ligase that specifically binds the C1A domain of PKC isozymes and causes their ubiquitination and degradation. The protein, named RINCK (RING protein that interacts with C kinase) was identified in a yeast two-hybrid screen for binding partners of PKCβ. We show that the protein causes the ubiquitination of PKCβII, but not the related kinase protein kinase A, *in vitro* and that it ubiquitinates PKC isozymes in cells. Knockdown experiments show that RINCK controls the stability of PKC by a mechanism distinct from that driving phorbol ester-mediated down-regulation. Rather, RINCK sets the level of PKC in the cell, thus controlling the amplitude of signaling by PKC.

EXPERIMENTAL PROCEDURES

Materials and Antibodies—The large T-antigen-transformed human embryonic kidney cells (tsA201) were the generous gift of Dr. Marlene Hosey (Northwestern University). The cDNA of rat PKCβII was a gift of Dr. Daniel E. Koshland, Jr. (University of California, Berkeley), and the cDNA of rat PKCα was a gift of Dr. Alex Toker (Harvard Medical School). The cDNA of HA-ubiquitin was a gift of Dr. Clive Palfrey (University of Chicago). Purified PKA was a gift from Dr. Susan Taylor (University of California, San Diego). Protein phosphatase 1 (PP1) and MG132 were obtained from Calbiochem. PKCα and βII were purified from the baculovirus expression system, as previously described (21). A polyclonal antibody against PKCβII (C-18, α-PKCβII) and a polyclonal antibody against PKCα (C-20, α-PKCα) were purchased from Santa Cruz Biotechnology. A monoclonal antibody against a determinant in the regulatory domain of PKCα was purchased from Transduction Laboratories. PDBu, *N*-ethylmaleimide, antibodies to α-tubulin, and FLAG epitope were obtained from Sigma. A monoclonal antibody against ubiquitin was purchased from Zymed Laboratories Inc.. The polyclonal anti-RINCK antibody was produced in two rabbits with His-RING (residues 20–210 in RINCK) as an antigen (Strategic Biosolutions, DE).

Yeast Two-hybrid Screen—The cDNA encoding the NH_2-terminal tail of rat PKCβII (residues 1–111) was amplified by PCR and inserted into the NcoI (5′ site) and BamHI sites (3′ site) of pAS2.1 (Clontech). The resulting plasmid was used as bait to screen a cDNA library derived from 9.5- and 10.5-day-old mouse embryos (22). Approximately 100,000 yeast CG1945 transformants were grown in the absence of tryptophan, leucine, and histidine at 30 °C for 8 days. Colonies that grew in this minimal selective media condition were scored for β-galactosidase activity by colony lift assay according to the Clontech MatchMaker protocol. Prey plasmid DNA from the double-positive ($His^+/LacZ^+$) colonies was rescued by electroporation into *Escherichia coli* HB101 (Invitrogen) and then retransformed back into yeast strain SFY526 containing the original bait plasmid and various control plasmids for one-to-one interactions. Both strands of the DNA insert from these clones were sequenced by automated sequencing (DNA Sequencing Shared Resource, Cancer Center, University of California, San Diego).

cDNA Cloning—The full-length RINCK1 and RINCK2 were PCR amplified from human heart total cDNA (Clontech) by using primers in 5′- and 3′-untranslated regions. The PCR products were cloned into TA cloning vector (Promega) and sequenced by automated sequencing.

Northern Blotting Analysis—A multiple tissue blot of human poly(A)$^+$ RNA (Clontech) was probed with random-primed ^{32}P-labeled DNA probes containing the original cDNA fragment that was obtained from the yeast two-hybrid screen. Hybridization was carried out at 68 °C by using ExpressHyb solution (Clontech), and the blot was washed under high stringency conditions (0.1 × SSC, 0.1% SDS at 50 °C).

Plasmid Constructs and Mutagenesis—The cDNAs encoding RINCK1 and RINCK2 were subcloned into pCMV-3FLAG vector (Sigma) for expression in mammalian cells following PCR amplification of the relevant sequences using pTA-RINCK1/RINCK2 as templates. Specifically, the primers used for the PCR amplification introduced an EcoRI site and a BamHI site at the 5′ and 3′ ends, respectively. The PCR products were subcloned into the pCMV-3FLAG vector digested with EcoRI and BamHI. The C20A point mutations in RINCK1/RINCK2 were generated by site-directed mutagenesis (Stratagene) according to the manufacturer's protocol. The cDNA encoding the wild-type PKCβII was subcloned into the pcDNA3 vector for expression in mammalian cells (23). The pseudosubstrate region (N-PS, residues 1–31), the C1A domain (N-C1A, residues 1–111), the C1 domain (N-C1, residues 1–170), and the C2 domain (C2, residues 171–288) were expressed as glutathione *S*-transferase (GST) fusion proteins in mammalian cells following PCR amplification of the relevant sequences using pcDNA3-PKCβII as the template. Specifically, the primers used for the PCR amplification introduced a BamHI site and a ClaI site at the 5′ and 3′ ends, respectively. The PCR products were subcloned into the pEBG vector (a Gift from Dr. Bruce Mayer at University of Connecticut Health Center) digested with BamHI and ClaI.

In Vitro Pull-down Assay—The coding region of RINCK was cloned into pGEX-KG (Amersham Biosciences), and GST fusion proteins were expressed in *E. coli* BL21, purified, and immobilized on glutathione-Sepharose beads (Amersham Bio-

sciences) as described in Amersham Biosciences instruction manual. 0.5 μg of pure PKCβII/α was incubated with 0.5 μg of fusion protein immobilized on glutathione-Sepharose beads in phosphate-buffered saline, pH 7.4, 1% Triton X-100 overnight at 4 °C with gentle rocking. Beads were then washed twice with the incubation buffer, 500 mM NaCl and twice with the incubation buffer. Bound proteins were eluted with sample buffer, analyzed by SDS-PAGE and immunoblotting.

Cell Culture, Transfection, and Treatment—HEK, tsA201, HeLa, COS7, H157, MCF7 and C2C12 cells were maintained in Dulbecco's modified Eagle's medium (Invitrogen) containing 10% fetal bovine serum (Invitrogen) at 37 °C in 5% CO_2. Transient transfection of tsA201 cells was carried out using Effectene transfection reagents (Qiagen). The specific transfection procedures were performed according to the protocol suggested by Qiagen using 1 μg of DNA. For siRNA studies, HeLa cells were transfected with 200 nM control nonspecific siRNA or siRNAs against 4 different regions in RINCK (combination of 50 nM each) (Dharmacon) using Lipofectamine2000 (Invitrogen). The siRNA sequences (Set 1) were: 1) ATATGGTCCAGGTGATTCG; 2) AAGGAGACTTTCAATAGGTGT; 3) AATGAGCCGGATGTTCTGT; and 4) CAGACCGGCCAGAATTTAG. In addition, H157 and MCF7 cells were similarly transfected with SmartPool siRNA (Set 2, a different set of 4 sequences; Dharmacon). These sequences were: 1) CAAUAGGUGUGAAGAGGUAUU; 2) CCQQUAUGGUCCAGGUGAUUU; 3) GAGAUGAGUUAGAUCGGGAUU; and 4) UAGCUUCACUUGAGAGAGAUU. Cells were harvested 3 days after transfection. For MG132 experiments, cells were treated with 10 μM MG132 or Me_2SO for 6 h. For PKC degradation with siRNA and PDBu experiments, HeLa cells were transfected with siRNAs and incubated for 3 days and treated with 200 nM PDBu for various times.

In Vivo GST Fusion Protein Pull-down Assay—To map the binding region of PKCβII to RINCK *in vivo*, the N-PS region, the N-C1A region, the C1 domain, and the C2 domain of PKCβ were expressed as GST fusion proteins in tsA201 cells together with FLAG-tagged RINCK. Approximately 40 h post-transfection, the transfected cells were lysed in buffer A (50 mM Tris-HCl, pH 7.5, 150 mM NaCl, 5 mM EDTA, 1% Triton X-100, 1 mM dithiothreitol, 2 mM benzamidine, 10 μg/ml leupeptin, 1 mM phenylmethylsulfonyl fluoride, and 100 nM microcystin-LR). The lysate was cleared by centrifugation at 13,000 × *g* for 10 min at 4 °C and the resulting supernatant is referred to as the detergent-solubilized cell lysate. Five percent of the total cell lysate was kept in SDS sample buffer for further analysis, and the remaining whole cell lysate was incubated with glutathione-Sepharose overnight at 4 °C. After washing three times in buffer B (Buffer A plus 300 mM NaCl) and once in buffer A, the glutathione-Sepharose bound proteins were analyzed using SDS-PAGE and immunoblotting.

Immunoprecipitation—COS7 or tsA201 cells were transiently transfected with the constructs indicated in figure legends. About 40 h post-transfection, cells were lysed in buffer A or slightly modified buffer C (50 mM Tris-HCl, pH 7.4, 100 mM NaCl, 5 mM EDTA, 1% Triton X-100, 10 mM sodium pyrophosphate, 1 mM phenylmethylsulfonyl fluoride, 1 mM sodium vanadate). Five percent of the total detergent-solubilized cell lysate was quenched in SDS sample buffer for further analysis, and the remaining detergent-solubilized cell lysate was incubated with appropriate monoclonal or polyclonal antibody and Ultra-link protein A/G-agarose (Pierce) overnight at 4 °C. The immunoprecipitates were washed three times in buffer B and once in buffer A for PKCα immunoprecipitates and three times in Buffer C for all other immunoprecipitates. The proteins in the immunoprecipitates (entire sample) were separated using SDS-PAGE and analyzed using immunoblotting.

Protein Purification and in Vitro Ubiquitination Assays—The coding regions of RINCK1, RINCK1 C20A, RINCK2, or RINCK2 C20A were cloned into pGEX-KG (Amersham Biosciences), and GST fusion proteins were expressed in *E. coli* BL21, purified, and immobilized on glutathione-Sepharose beads (Amersham Biosciences) as described in the manufacturer's instructions. Assays for *in vitro* ubiquitination were carried out as described previously (24). Briefly, 0.5 μg of His-E1 (human) (25), 1 μg of His-UBC4 (human) (25), 2.5 μg of ubiquitin (bovine, Sigma), 2.5 μg of GST fusion protein of RINCK, and the indicated amount of PKCβII were incubated at 30 °C for 90 min in 2 mM ATP, 50 mM Tris-HCl, pH 7.5, 2.5 mM $MgCl_2$, and 0.5 mM dithiothreitol. Samples were boiled in SDS sample buffer and subjected to SDS-PAGE. Ubiquitin immunoblots were analyzed as described (26). For some experiments, 1 μg of PKCβII was treated with 312.5 units ml^{-1} PP1 for 30 min at room temperature to dephosphorylate PKC. In some cases, samples were diluted with 100 μl of buffer A containing 1% SDS after the *in vitro* ubiquitination assay and boiled for 5 min at 95 °C to dissociate protein complexes. Boiled samples were then diluted with 900 μl of buffer A and immunoprecipitated with antibodies against PKC by incubation at 4 °C overnight.

Cellular Ubiquitination Assays—TsA201 cells were transfected following a standard calcium phosphate co-precipitation procedure. The amounts of DNA used were 5 μg of PKC, 1 μg of HA-ubiquitin, or 0.5 μg of FLAG-RINCK1 constructs. Cells were treated with 10 μM MG132 for 6 h before harvest; some of them were treated with 200 nM PDBu for 30 min. Cells were harvested in buffer A with 10 mM *N*-ethylmaleimide to preserve ubiquitinated species. After centrifugation at 13,000 × *g* for 10 min, the supernatants were incubated with an anti-PKCα antibody (Transduction Laboratories) overnight at 4 °C, and Ultra-link protein A/G beads for 1 h. The immunocomplexes were washed three times with buffer B with 10 mM *N*-ethylmaleimide and once with buffer A with 10 mM *N*-ethylmaleimide.

Cell Fractionation—C2C12 cells were harvested in buffer A without 1% Triton X-100. After centrifugation at 13,000 × *g* for 30 min, the pellet was resuspended in buffer A. The supernatant is assigned as the cytosol. After the second centrifugation, the supernatant, the detergent-soluble fraction, is assigned as membrane and the pellet is the detergent-insoluble fraction.

RESULTS

Identification of RINCK—To identify novel PKC-binding proteins, we used a yeast two-hybrid approach to screen a mouse embryonic cDNA library with a sequence encoding the first 111 amino acids of rat PKCβ as bait. This sequence encodes the N-terminal tail, the pseudosubstrate sequence, and C1A domain of PKCβ. Five positive clones were obtained from

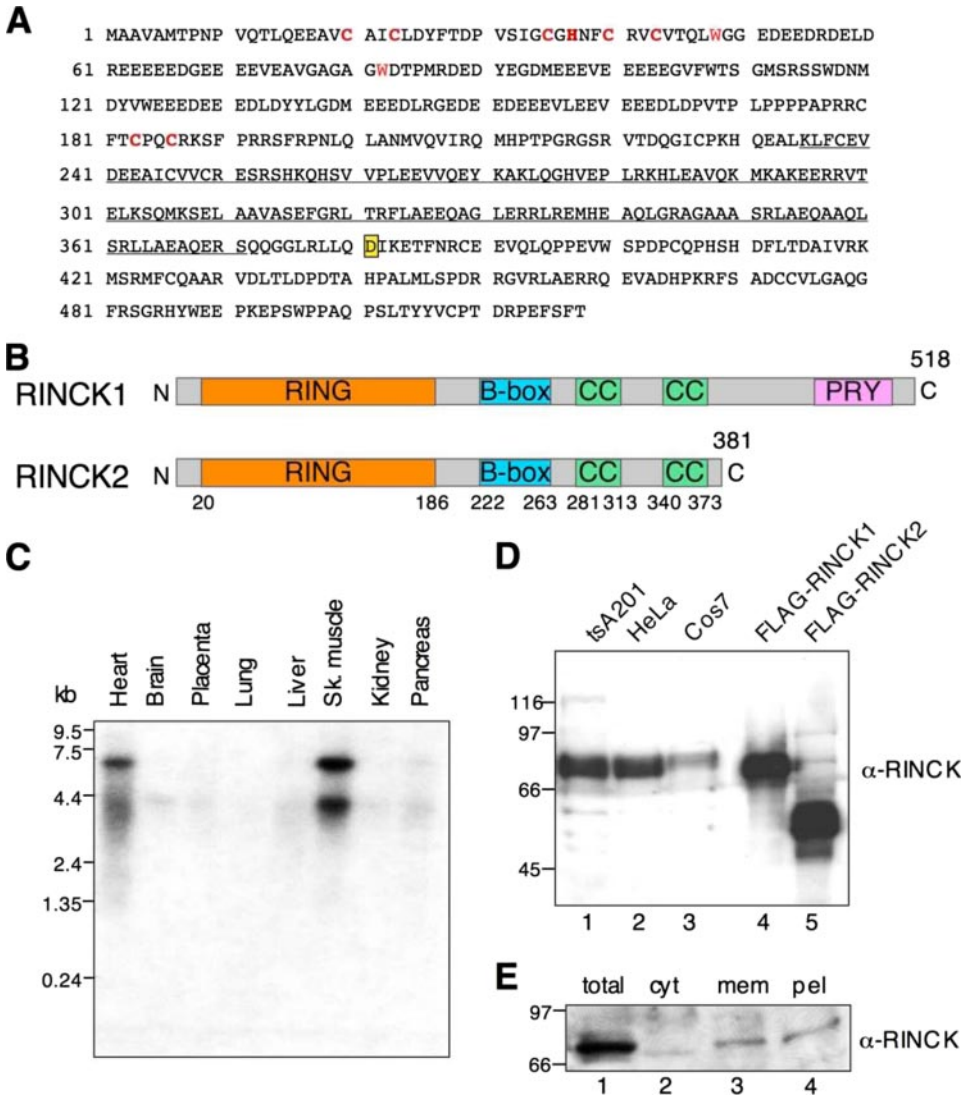

FIGURE 1. **Domain structure and characterization of RINCK.** *A*, amino acid sequence of RINCK. The sequence of the clone isolated in the initial yeast two-hybrid screen is identified by a *solid underline*. Conserved RING domain residues are indicated in *red*. The aspartic acid at residue 381 is boxed in *yellow*. There is a valine at this position in RINCK2 preceding an early stop codon. *B*, schematic diagram of the predicted domains in the two alternative splicing forms, RINCK1 and RINCK2. *CC*, coiled-coil region. *C*, Northern blot analysis of human RINCK mRNA. A multiple tissue blot of human poly(A)$^+$ mRNA was probed with a cDNA fragment of mouse RINCK labeled with [α-^{32}P]dCTP. Tissue sources of the poly(A)$^+$ mRNA are shown at the *top*, and the positions of markers are indicated on the *left*. Two transcripts of around 4 and 7 kb were detected with the highest expression levels in skeletal muscle and heart. *D*, FLAG-RINCK1 and FLAG-RINCK2 were overexpressed in tsA201 cells, respectively, and whole cell lysates were analyzed along with cell lysates of untransfected COS7, HeLa, and tsA201 cells by SDS-PAGE and Western blotting with an antibody against RINCK. *E*, C2C12 cells were fractionated into cytosol (*cyt*, *lane 2*), detergent-soluble membrane fraction (*mem*, *lane 3*), and detergent-insoluble pellet fraction (*pel*, *lane 4*), and analyzed by SDS-PAGE and immunoblotting.

~100,000 screened. One of these encoded a 72-amino acid sequence that data base analysis revealed was part of a novel gene predicted to encode a RING finger domain-containing protein. We named the putative protein RINCK for RING finger protein that interacts with C kinase (Fig. 1*A*).

The full-length RINCK cDNA was PCR amplified from human heart total cDNA. The first ATG in the RINCK cDNA complies with the Kozak rules and is preceded by an in-frame stop codon, located 63 bp upstream. The open reading frame of RINCK encodes a protein of 518 amino acids predicted to have a C3HC4-type RING finger, a Zn^{2+}-containing domain present in many E3 ubiquitin ligases (*orange*), a B-box (*blue*), and two coiled-coil regions (*green*) (Fig. 1*B*). These three domains define RINCK as being a member of the large (currently over 70 members identified) TRIM (tripartite motif) family of proteins (27, 28). These proteins have also been referred to as RBCC (RING-B-box-coiled-coil) proteins (29). In addition, RINCK contains a PRY domain, a segment of unknown function commonly found in TRIM proteins (Fig. 1*B*, *pink*). The human *RINCK* gene is located on chromosome 5 and contains eight coding exons. An alternatively spliced form of RINCK skips exon 4, causing a shift in reading frame that results in an Asp instead of Val at position 381 and an early stop directly after this residue (Fig. 1*A*, residue 381 *boxed* in *yellow*). We refer to the longer variant as RINCK1 and the shorter variant as RINCK2 henceforth. The original cDNA fragment we obtained from the yeast two-hybrid screen corresponds to residues 235–371 in RINCK (Fig. 1*A*, *underlined sequence*), which contains part of the B-box, the first coiled-coil region, and part of the second coiled-coil region. Northern blot analysis showed that the RINCK probe hybridized to two bands of 4- and 7-kb transcripts in multiple human tissues with the highest levels in heart and skeletal muscle (Fig. 1*C*). Following our cloning and initial characterization of RINCK1, Hanai and co-workers (30) reported on the cloning of two members of the TRIM (tripartite motif) family of proteins that correspond to the RINCK subfamily. Specifically, they identified TRIM41β, which corresponds to RINCK1 and a larger splice variant (COOH-terminal extension resulting in 630 residue protein), which they refer to as TRIM41α (30). Taken together with our work, and supported by sequences in the EST data base, there are thus three splice variants of RINCK: 381 amino acids (RINCK 2), 518 amino acids (RINCK1/TRIM 41β), and 630 amino acids (TRIM41α). Given the role of these proteins in controlling PKC (see below), we retain the RINCK nomenclature.

To examine the expression of endogenous RINCK protein, a polyclonal antibody was raised against a fusion protein comprising residues 20–210 of RINCK fused to an amino-terminal His tag. The Western blot in Fig. 1*D* shows that this antibody detected an ~80-kDa protein in tsA201 cells transfected with

the cDNA for FLAG-tagged RINCK1 (*lane 4*) and an ~50-kDa protein in cells transfected with the cDNA for FLAG-tagged RINCK2 (*lane 5*). The antibody detected a band co-migrating with recombinant RINCK1, but not RINCK2, in tsA201, HeLa, and COS7 cells (Fig. 1*D*, *lanes 1–3*, respectively). Fractionation of C2C12 cells revealed that endogenous RINCK1 partitioned equally between the detergent-soluble membrane fraction (Fig. 1*E*, *lane 3*) and detergent-insoluble fraction (Fig. 1*E*, *lane 4*). A minor species of RINCK1 with a slightly faster mobility was detected in the cytosol (Fig. 1*E*, *lane 2*). These data reveal that RINCK1 is the major species expressed in cells, where it partitions equally between the membrane and detergent-insoluble fractions. In subsequent studies, we focused on RINCK1 because it is the predominant isoform.

RINCK Interacts with PKC in Cells—We next asked whether PKC interacts with RINCK in cells. TsA201 cells were co-transfected with the cDNA for PKCα and FLAG-tagged RINCK1. RINCK1 was immunoprecipitated from the detergent-solubilized fraction of cell lysates using an anti-FLAG antibody and the immunoprecipitate was analyzed for bound PKCα by Western blot analysis. Fig. 2*A* reveals that recombinant PKCα was present in immunoprecipitates of FLAG-RINCK1 (*lane 3*) but not control immunoprecipitates in which lysate was incubated with control IgG (*lane 2*). Conversely, FLAG-RINCK1 associated with immunoprecipitated PKCα from tsA201 cells co-transfected with PKCα and RINCK1 (data not shown). We next asked whether endogenous RINCK and endogenous PKCα interact in cells. RINCK was immunoprecipitated from tsA201 cells and probed for bound PKCα. A discrete band co-migrating with PKCα was visible in Western blots of immunoprecipitated RINCK (Fig. 2*B*, *lane 3*), but not control beads incubated with preimmune serum (Fig. 2*B*, *lane 2*). Thus, RINCK forms a complex with PKCα in cells.

To examine whether PKC binds RINCK directly, we performed an *in vitro* GST pull-down assay using recombinant PKCα purified from baculovirus-infected insect cells and either GST alone or a GST fusion protein of RINCK1 purified from bacteria. Proteins bound to glutathione-Sepharose beads were identified by Western blot analysis using an antibody against PKCα. Fig. 2*C* shows that PKCα bound to GST-RINCK1 (*lane 2*) but not to GST alone (*lane 1*), revealing that PKCα binds to RINCK directly.

We next explored whether the interaction of RINCK with PKC was isoform-specific or general to all PKC family members. TsA201 cells were transfected with the cDNAs encoding a PKC from each class: PKCβII (another conventional isozyme), PKCδ (novel), or PKCζ (atypical). The Western blot in Fig. 3 shows that all three isoforms were present in immunoprecipitates of FLAG-RINCK1 (*lane 2*) but not in controls. Binding to the conventional and novel PKC isoforms was significantly stronger than the binding to the PKCζ; nonetheless, weak binding to this isoform was consistently observed. These isoforms all contain a C1 domain, part of the bait used in the yeast two-hybrid screen that pulled out RINCK. Thus, we asked whether RINCK also bound non-PKC C1 domain-containing proteins. Fig. 3*D* shows that RINCK1 did not bind β2-chimaerin, another C1 domain containing protein. These data reveal that RINCK specifically binds PKC isoforms, but does not bind β2-chimaerin, a protein that also has a C1 domain.

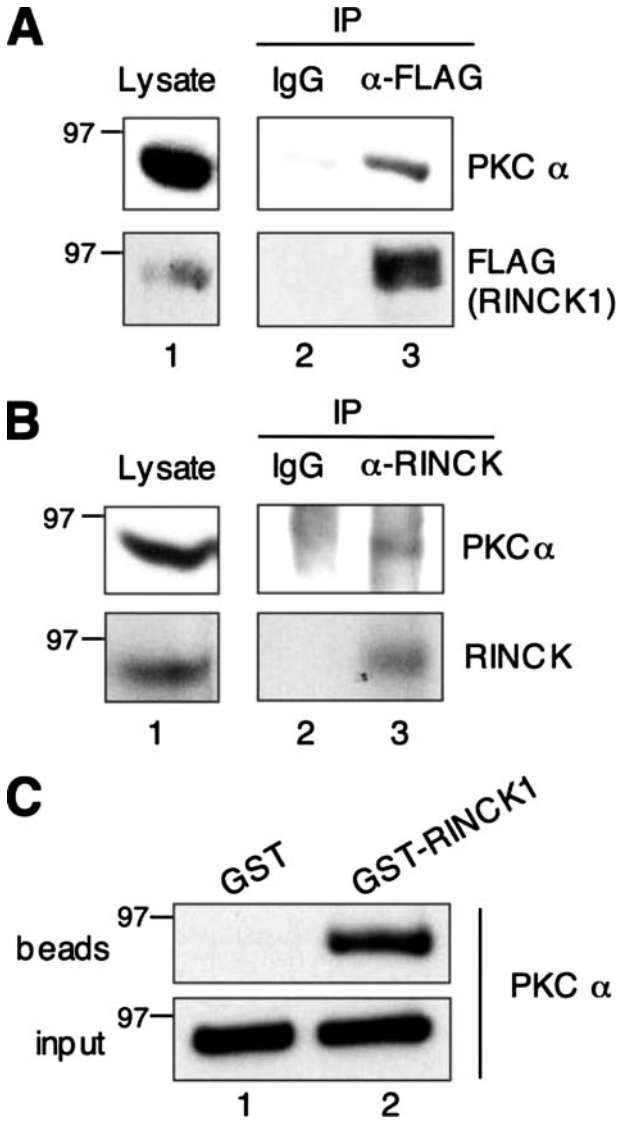

FIGURE 2. **The interaction between RINCK and PKCα.** *A*, FLAG-RINCK1 and PKCα were co-expressed in tsA201 cells, RINCK1 was immunoprecipitated (*IP*) with the anti-FLAG antibody, and the immunoprecipitates analyzed by Western blot with the indicated antibodies. 5% of the lysate (*lane 1*) and the entire immunoprecipitate (*lanes 2* and *3*) were analyzed. *B*, Western blot of detergent-solubilized lysate of tsA201 cells probed with anti-PKCα antibody or anti-RINCK antibody (*lane 1*). Endogenous RINCK was immunoprecipitated from the detergent-solubilized lysate using α-RINCK antibody, and probed for PKCα (*lane 3*); preimmune sera were used in control immunoprecipitation (*lane 2*). 5% of the lysate (*lane 1*) and the entire immunoprecipitate (*lanes 2* and *3*) were analyzed. *C*, PKCα directly binds RINCK1 *in vitro*. Purified PKCα (0.1 μg/μl) was incubated with GST or GST-RINCK1 immobilized on glutathione-Sepharose at 4 °C for 1 h. After washes, the proteins that bound to the glutathione beads were separated by SDS-PAGE and probed with the polyclonal anti-PKCα antibody.

The C1A Domain of PKCβII Mediates the Interaction with RINCK—The bait used in the yeast two-hybrid screen comprised the first 111 amino acids of PKCβII, which includes the pseudosubstrate sequence and C1A domain. To further delineate the binding site for RINCK in PKC, we expressed a series of GST-tagged constructs of the amino terminus of PKCβII: N-PS (first 31 residues containing the pseudosubstrate); N-C1A (first 111 residues up to and including the C1A domain); N-C1 (first

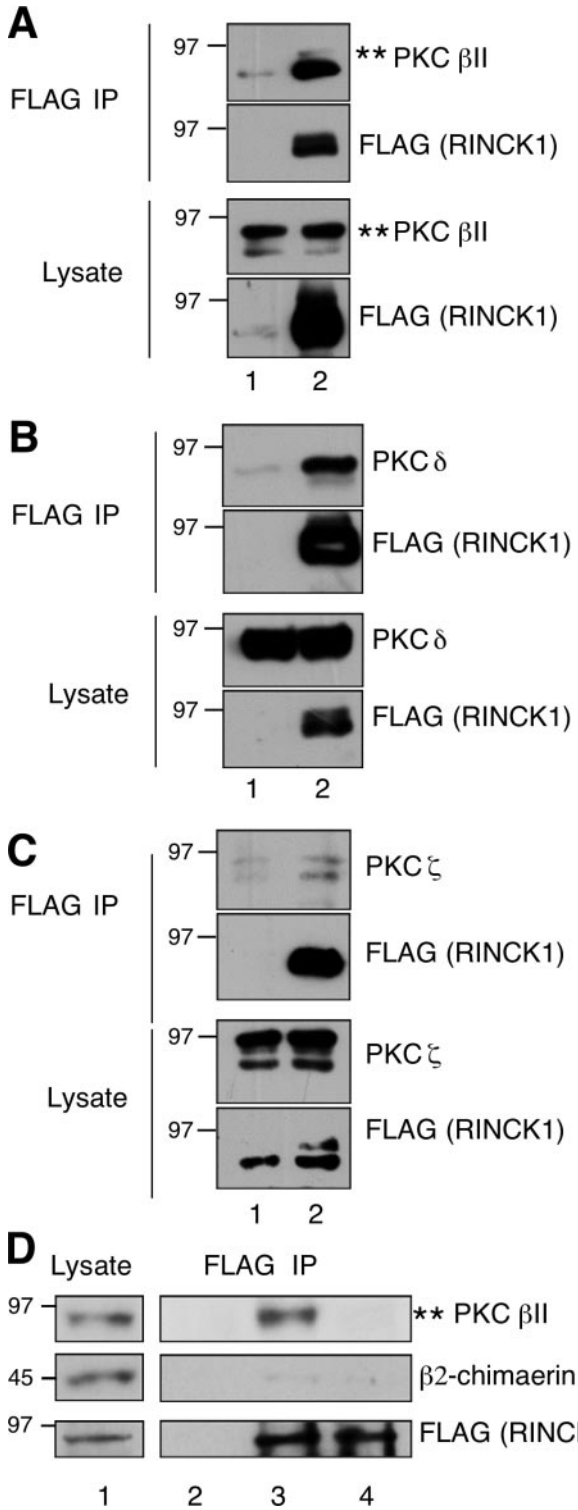

FIGURE 3. **Interactions between RINCK and PKC isozymes.** *A*, PKCβII was co-expressed with control vector or FLAG-RINCK1 in COS7 cells, and immunoprecipitation (*IP*) with the anti-FLAG antibody was performed before immunoblotting with the indicated antibodies. *Double asterisk* indicates position of mature (phosphorylated) PKCβII. *B*, PKCδ was co-expressed with control vector or FLAG-RINCK1 in COS7 cells, and immunoprecipitation with the anti-FLAG antibody was performed before immunoblotting with the indicated antibodies. *C*, PKCζ was co-expressed with control vector or FLAG-RINCK1 in COS7 cells, and immunoprecipitation with the anti-FLAG antibody was performed before immunoblotting with the indicated antibodies. Note FLAG-RINCK1 is the major lower band on this blot. *D*, PKCβII or β2-chimaerin were co-expressed with FLAG-RINCK1 in tsA201 cells, and immunoprecipitation with the anti-FLAG antibody was performed before immunoblotting with the indicated antibodies.

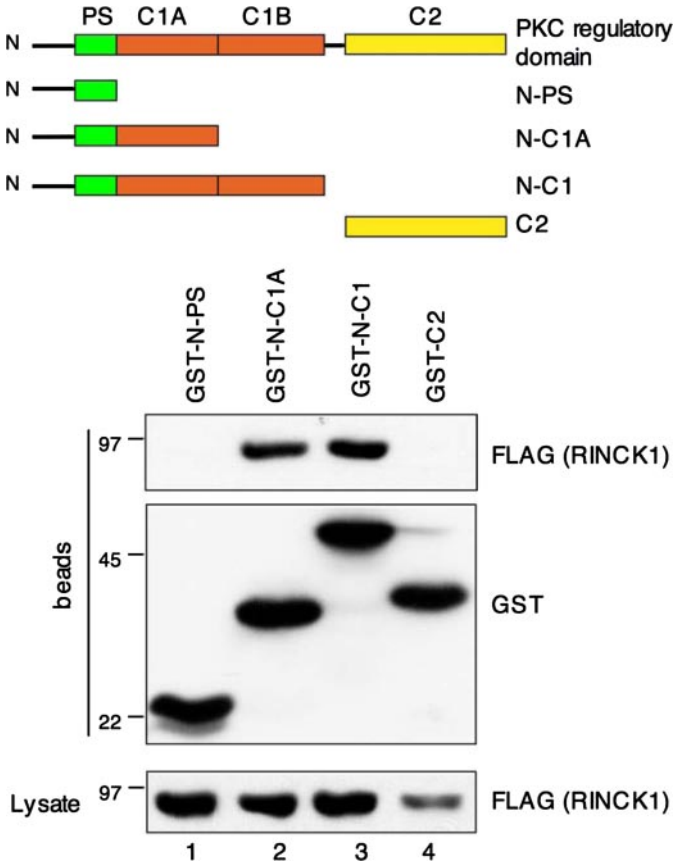

FIGURE 4. **The C1A domain of PKCβII mediates its interaction to RINCK1 *in vivo*.** The indicated GST-tagged fusion proteins encoding different domains of PKCβII were co-expressed with the FLAG-tagged RINCK1 in tsA201 cells: GST vector, GST-N-PS, GST-N-C1A, GST-N-C1, and GST-C2 (see "Experimental Procedures"). Detergent-solubilized cell lysates were incubated with glutathione-Sepharose to precipitate the GST fusion proteins. The proteins that bound to the glutathione beads were analyzed using SDS-PAGE and immunoblotting.

170 residues); and C2 (residues 171–288) (Fig. 4). FLAG-RINCK1 was co-expressed with these GST-tagged constructs in tsA201 cells, the expressed GST fusion proteins were immobilized to glutathione-Sepharose beads, and bound RINCK was detected using the anti-FLAG antibody. The expression level of RINCK transfected with different constructs is shown in the *bottom panel* of Fig. 4. All GST-tagged constructs were expressed in tsA201 cells and effectively precipitated by glutathione-Sepharose beads (Fig. 4, *upper panel*) as judged by staining with anti-GST antibodies. RINCK1 associated with all the PKC constructs that contained the C1A domain: GST-N-C1A (*lane 2*) and GST-N-C1 (*lane 3*). It did not interact with the construct lacking the C1A domain, GST-N-PS (*lane 1*,) or the C2 domain, GST-C2 (*lane 4*). Furthermore, similar interaction was observed to the amino-terminal constructs containing just the C1A domain (*lane 2*) or the C1A and C1B domains (*lane 3*). These data suggest that the C1A domain in the regulatory moiety of PKCβII provides the primary determinants in the interaction of PKC with RINCK.

RINCK Contains Intrinsic RING-dependent E3 Ubiquitin Ligase Activity and Promotes the Ubiquitination of PKCβII in Vitro—Sequence analysis revealed that RINCK is predicted to encode a RING finger domain; this domain has been shown to

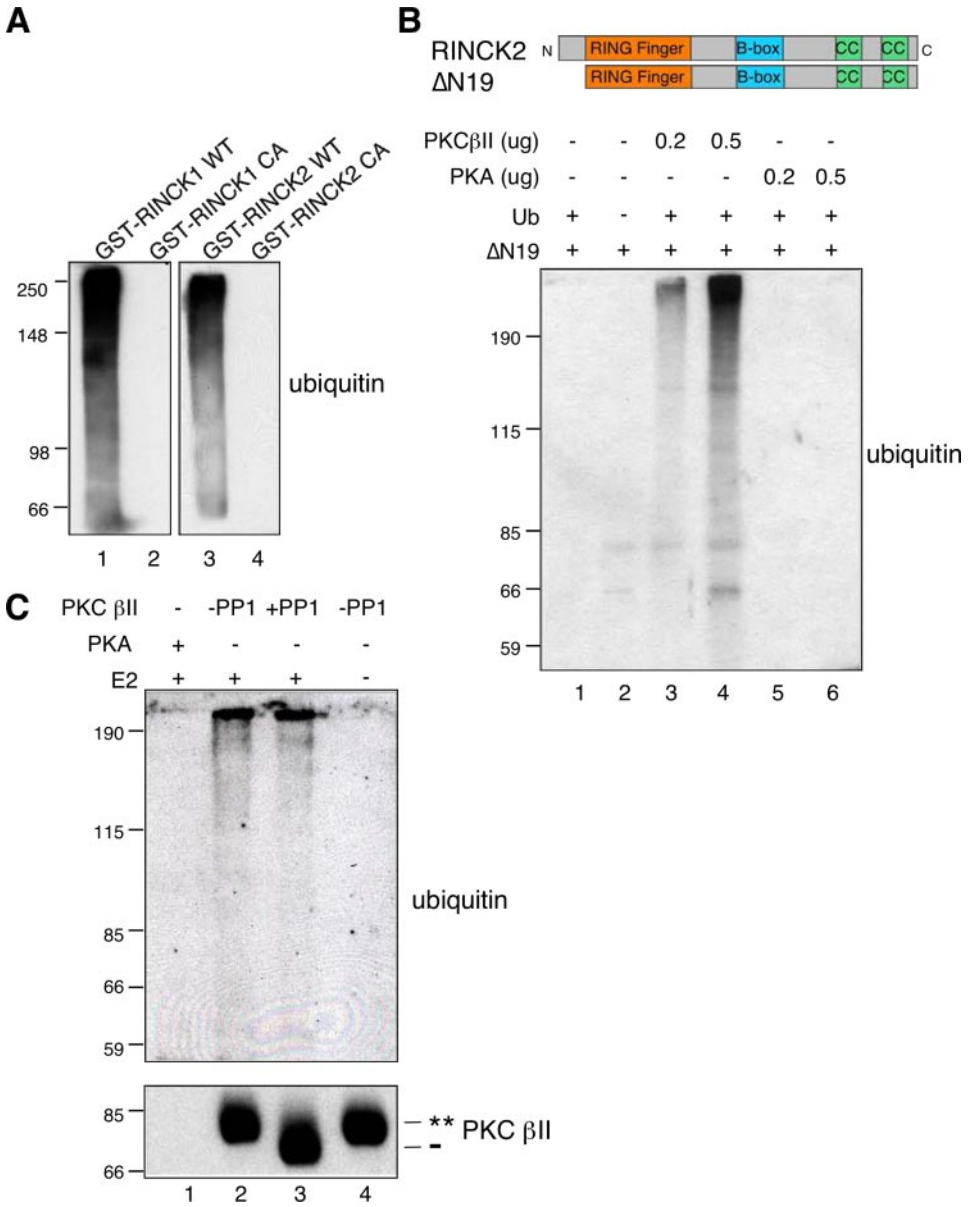

FIGURE 5. **RINCK contains intrinsic RING-dependent E3 ubiquitin ligase activity and promotes the ubiquitination of PKCβII *in vitro*.** *A*, RINCK1 and RINCK2 have RING-dependent intrinsic E3 ligase activities *in vitro*. Purified recombinant E1, E2, and GST-RINCK1 wt/CA (C20A) or GST-RINCK2 wt/CA (C20A) were incubated with ATP and ubiquitin (*Ub*) at 30 °C for 90 min. The reaction mixture was then subjected to anti-ubiquitin immunoblotting. *B*, RINCK promotes the ubiquitination of PKCβII *in vitro*. GST-RINCK2-ΔN19 was incubated with or without ubiquitin (*lanes 1* and *2*), with 0.2 or 0.5 μg of purified PKCβII (*lanes 3* and *4*), and 0.2 or 0.5 μg of purified PKA (*lanes 5* and *6*), together with E1, E2, and ATP at 30 °C for 90 min. The reaction mixtures were then subjected to SDS-PAGE and anti-ubiquitin immunoblotting. *C*, RINCK promotes the ubiquitination of both phosphorylated and dephosphorylated PKCβII *in vitro*. GST-RINCK2-ΔN19 was incubated with purified PKA (*lane 1*), purified PKCβII pretreated without or with PP1 (*lanes 2* and *3*) together with E1, E2, and ATP, or with PKCβII, E1, and ATP (*lane 4*) at 30 °C for 90 min. The reaction mixtures were then subjected to SDS-PAGE and anti-ubiquitin immunoblotting.

confer intrinsic E3 ubiquitin ligase activity to a number of proteins (16, 29). Thus, we asked whether RINCK contains intrinsic E3 ubiquitin ligase activity and whether it depended on a functional RING finger domain. In many RING finger E3 ubiquitin ligases, mutation of the first cysteine of the RING finger disrupts the domain structure and the ubiquitin ligase activity (16, 29). To investigate whether the E3 ubiquitin ligase activity of RINCK is RING-dependent, we introduced the equivalent mutation into RINCK1 and RINCK2 (C20A; first Cys highlighted in *red* in the sequence in Fig. 1*A*). Autoubiquitination of RINCK was examined by incubating purified GST fusion proteins of either wild-type or CA mutants of RINCK1 or RINCK2 with purified ubiquitin-activating enzyme His-E1, ubiquitin-conjugating enzyme His-E2 (Ubc4), ubiquitin, and ATP. The Western blot in Fig. 5*A* shows that anti-ubiquitin antibodies labeled higher molecular weight species following reaction with wild-type RINCK1 and RINCK2 (*lanes 1* and *3*, respectively) but not with the CA mutants of either protein (*lanes 2* and *4*, respectively). These data suggest that RINCK has E3 ubiquitin ligase activity *in vitro* and that this activity is abolished by mutation of the first conserved Cys in the domain to Ala.

Next, we determined whether PKCβII could be ubiquitinated by RINCK *in vitro*. In this experiment, we used a truncated GST fusion protein of RINCK2, ΔN19, which has the first 19 amino acids missing but the RING finger domain intact. Unlike full-length RINCK, ΔN19 does not self-ubiquitinate (Fig. 5*B*, *lanes 1* and *2*). Addition of increasing amounts of pure PKCβII to the ubiquitination assay resulted in the appearance of high molecular weight species labeled with the anti-ubiquitin antibody (Fig. 5, *lanes 3* and *4*). These species were absent when E2 was omitted from the reaction mixture. In contrast, no such labeling was detected when increasing amounts of purified PKA were incubated with ΔN19 (Fig. 5*B*, *lanes 5* and *6*). Ubiquitinated PKC was still detectable in anti-PKC immunoprecipitates from boiled samples in the presence of SDS, which disrupts protein-protein interactions (data not shown). These results indicate that RINCK specifically promotes the ubiquitination of PKCβII *in vitro*.

Degradation mechanisms have been proposed for both phosphorylated and dephosphorylated PKC (18), leading us to ask whether RINCK discriminates between phosphorylated PKC and dephosphorylated PKC. PKCβII purified using baculovirus expression in insect cells is phosphorylated at all three maturation sites: the activation loop, the turn motif, and the hydrophobic motif. Treatment with PP1 dephosphorylates all three sites,

resulting in a protein with a faster electrophoretic mobility (31). Thus, purified PKCβII was treated without or with PP1 to dephosphorylate the kinase and then incubated with ΔN19 in *in vitro* ubiquitination assays. Fig. 5*C* shows that PP1-treated PKCβII ran as a faster migrating band (*lane 3*, species labeled with *dash*) compared with untreated PKCβII (*lanes 2* and *4*, species labeled with *two asterisks*), consistent with quantitative dephosphorylation of the kinase. *In vitro* ubiquitination assays revealed that RINCK promoted the ubiquitination of both species equally well: similar amounts of ubiquitin-labeled higher molecular weight species were detected using phosphorylated and dephosphorylated PKCβII as substrate (Fig. 5*C*, *lanes 2* and *3*). No ubiquitination was observed when PKA was used as substrate (*lane 1*) or when E2 was omitted from the reaction mixture (*lane 4*). In addition, RINCK promoted similar levels of ubiquitination of PKCβII in the presence or absence of activating cofactors (phosphatidylserine, diacylglycerol, and Ca^{2+}) (data not shown). These data reveal that RINCK promotes the ubiquitination of PKC independently of the phosphorylation or activation state of the kinase.

Overexpression of RINCK Promotes the Ubiquitination of PKCβII in Cells—Next, we asked whether RINCK ubiquitinates PKC in cells. PKCβII was co-expressed in tsA201 cells with HA-ubiquitin and either wild-type FLAG-RINCK1 or FLAG-RINCK1 CA. Because phorbol ester treatment has been previously shown to promote the ubiquitination of PKC (13), we also compared the effects of treating cells with or without PDBu for 30 min prior to harvest. PKCβII was immunoprecipitated with an anti-PKCβII antibody followed by immunoblotting with an anti-HA antibody to detect ubiquitin-conjugated PKCβII (Fig. 6). Increased levels of HA-tagged ubiquitin were detected on PKCβII in the presence of exogenous RINCK (Fig. 6, *lane 2*), indicating that RINCK promotes the ubiquitination of PKCβII. The RINCK-mediated ubiquitination is likely to be polyubiquitination, because the ubiquitinated PKCβII was detected as a high molecular weight smear. We also examined the effect of the C20A mutant of RINCK on the ubiquitination PKCβII in cells. Introduction of this point mutation in the RING finger domain of RINCK abolished the ability of RINCK to ubiquitinate PKCβII (Fig. 6, *lane 3*), providing further evidence to support the role of RINCK as a RING E3 ubiquitin ligase for PKC. Similar results were been observed for PKCα (data not shown). As reported previously, treatment of control cells caused a small increase in the ubiquitination of PKCβII (19) (Fig. 6, *lane 4*). However, this PDBu-induced increase was not enhanced in cells overexpressing RINCK1 indicating that RINCK does not significantly facilitate the phorbol ester-mediated degradation. Thus, RINCK induces the ubiquitination of PKC by a pathway independent of the phorbol ester-mediated ubiquitination.

RINCK Targets PKC for Degradation in Cells—Polyubiquitination of a cellular protein typically leads to the degradation of the protein by the proteasome (32). To determine whether RINCK-mediated ubiquitination of PKC promotes its degradation, we measured the effect of overexpressing either wild-type or catalytically inactive (CA) RINCK on the levels of PKCβII; this isozyme was chosen for these experiments because of extensive studies characterizing its life cycle (reviewed in Ref. 33). The Western blot and accompanying graph in Fig. 7 shows

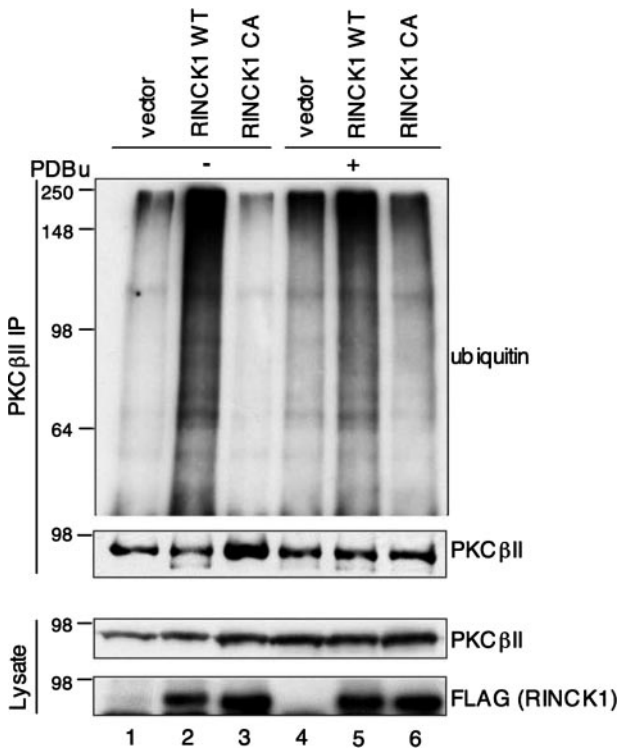

FIGURE 6. **Overexpression of RINCK1 promotes the ubiquitination of PKCβII *in vivo*.** FLAG-RINCK1 wt, FLAG-RINCK1 CA, or empty vector was overexpressed together with PKCβII and HA-ubiquitin in tsA201 cells. Cells were treated without or with 200 nM PDBu for 30 min prior to harvest. PKCβII was immunoprecipitated from cell lysates and the immunoprecipitated proteins were subjected to anti-HA immunoblotting.

that co-expression of wild-type RINCK1 caused a 3-fold reduction in the steady-state level of PKCβII compared with the levels in control cells (Fig. 7*A*, *lanes 1* and *2*). In contrast, overexpression of the C20A mutant of RINCK1 caused a 3-fold increase in the amount of PKCβII (Fig. 6*A*, *lane 3*). Similar results have been observed for PKCα (data not shown). Note that the expression level of wild-type RINCK1 was significantly less than that of the catalytically inactive CA construct, presumably because the wild-type enzyme was catalyzing its autoubiquitination and degradation (Fig. 7*A*, *lower panel*). It is also noteworthy that some variability in the effects of overexpression was observed (note smaller effects in Fig. 6*A*) and may relate to the levels of overexpression of the RINCK constructs. These data reveal that RINCK promotes the degradation of PKC, and that this degradation is prevented by a catalytically inactive construct of RINCK, which functions as a dominant-negative mutant of endogenous RINCK in cells.

We also addressed whether the degradation of PKC promoted by RINCK in cells depended on the phosphorylation state of PKC. To this end, we expressed a construct of PKCβII in which one of the autophosphorylation sites, Ser-660, is mutated to Ala. This construct is phosphatase-labile and as a consequence dephosphorylated species accumulate as evidenced by the faster migrating band in the Western blot in Fig. 7*B* (indicated with *dash*). Co-expression of wild-type RINCK1 reduced the levels of both phospho- (*asterisk* marks the migration position of PKCβII with one phosphate (the turn motif, Thr-641), on the COOH-terminal tail) and dephospho- (*dash*) PKC com-

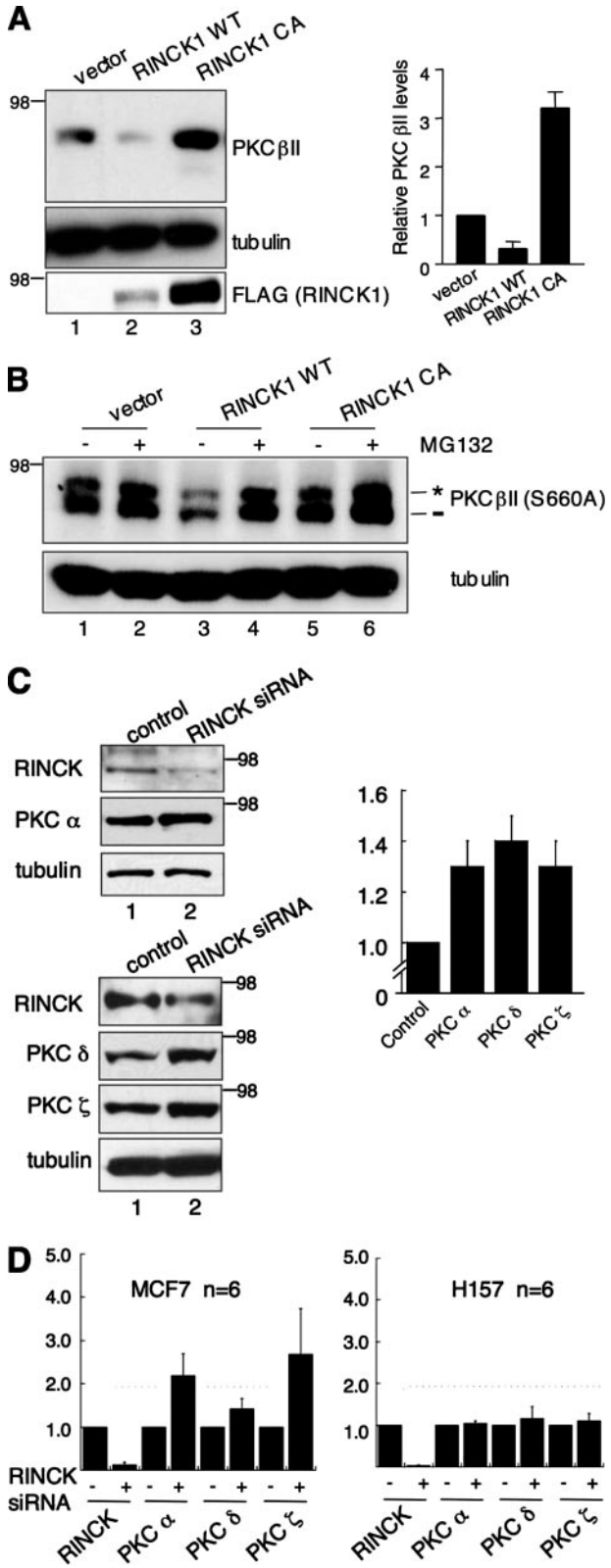

FIGURE 7. **RINCK targets PKC for degradation *in vivo*.** *A*, FLAG-RINCK1 wt, FLAG-RINCK1 CA, or empty vector was co-expressed with PKCβII in tsA201 cells and the level of PKCβII, RINCK1, and tubulin assessed by Western blot analysis. Quantified data from four independent experiments ± S.E. are shown on the *right*: levels of PKCβII in cells were normalized to those in cells transfected with empty vector. *B*, FLAG-RINCK1 wt, FLAG-RINCK1 CA, or empty vector was co-expressed with PKCβII S660A in tsA201 cells. Cells were treated with Me_2SO or 10 μM MG132 for 6 h before harvest. The total cell lysates were analyzed using SDS-PAGE and immunoblotting. *C*, control nonspecific siRNA or RINCK siRNA (Set 1 under "Experimental Procedures") were transfected into HeLa cells. The total cell lysates were analyzed using SDS-PAGE and immunoblotting. Quantification data on the *right* shows the relative protein level of endogenous PKC α, δ, and ζ in cells. Data represent the results from three independent experiments. *D*, *bar graph* showing effect of RINCK knockdown using Smart Pool siRNA (Set 2 under "Experimental Procedures") on PKCα, PKCδ, and PKCζ levels in MCF7 and H157 cell lines. Data represent the average ± S.E. of six independent experiments.

pared with vector-transfected cells. This reduction was prevented with the proteasome inhibitor MG132. Thus, the RINCK-mediated degradation of PKC is not sensitive to the phosphorylation state of the kinase in cells and is proteasome-dependent.

To further explore the role of RINCK in PKC degradation, we examined the effect of depleting endogenous RINCK on the levels of endogenous PKC isozymes in HeLa cells. The major conventional PKC isozyme in these cells is PKCα, so we focused on this isozyme. We also examined one novel (PKCδ) and one atypical (PKCζ) isozyme expressed in these cells. Treatment of cells with siRNAs targeted to RINCK caused a greater than 2-fold reduction in RINCK levels. Fig. 7*C* shows that the protein levels of endogenous PKCα, PKCδ, and PKCζ increased by ~40% in cells lacking RINCK (*lane 2*) compared with the control sample (*lane 1*).

To validate the siRNA results, we knocked down RINCK in two additional cell lines using a completely different set of three siRNAs (see "Experimental Procedures"). Fig. 7*D* shows that this additional set of siRNAs effectively knocked down RINCK in two cancer cell lines, the breast cell line MCF7 and the non-small cell lung carcinoma H157 cells. Analysis of data from six independent experiments revealed that RINCK knockdown caused a 2-fold increase in the levels of PKCα and PKCζ, in addition to a more modest increase in the levels of PKCδ. In contrast, knockdown in H157 cells did not significantly affect the levels of these three PKC isozymes. Taken together, these data reveal that RINCK differentially affects PKC levels in various cancer cell lines, with the most pronounced effects in MCF7 cells, intermediate effects in HeLa cells, and no detectable effects in H157 cells.

Lastly, we addressed whether RINCK participates in the phorbol ester-mediated down-regulation of PKC. Specifically, we measured the rate of phorbol ester-mediated degradation of endogenous PKCα in HeLa cells treated with control siRNA or RINCK-specific siRNA. Fig. 8 shows that PKCα levels were ~40% higher in cells depleted of RINCK compared with control cells. In addition, species of intermediately phosphorylated PKC were visible: both unphosphorylated (*dash*) and PKC phosphorylated at one C-terminal site (*asterisk*) were observed in cells depleted of RINCK. Treatment of control or RINCK-deficient cells with phorbol esters caused a disappearance of PKC in the detergent-soluble fraction, the classic down-regulation phenomenon. Importantly, the half-time of disappearance of PKC was comparable in control cells to ones depleted of RINCK (3.3 ± 0.9 and 3 ± 1 h, respectively). Thus, the phorbol ester-mediated degradation of PKC occurs independently of the RINCK-mediated degradation of PKC.

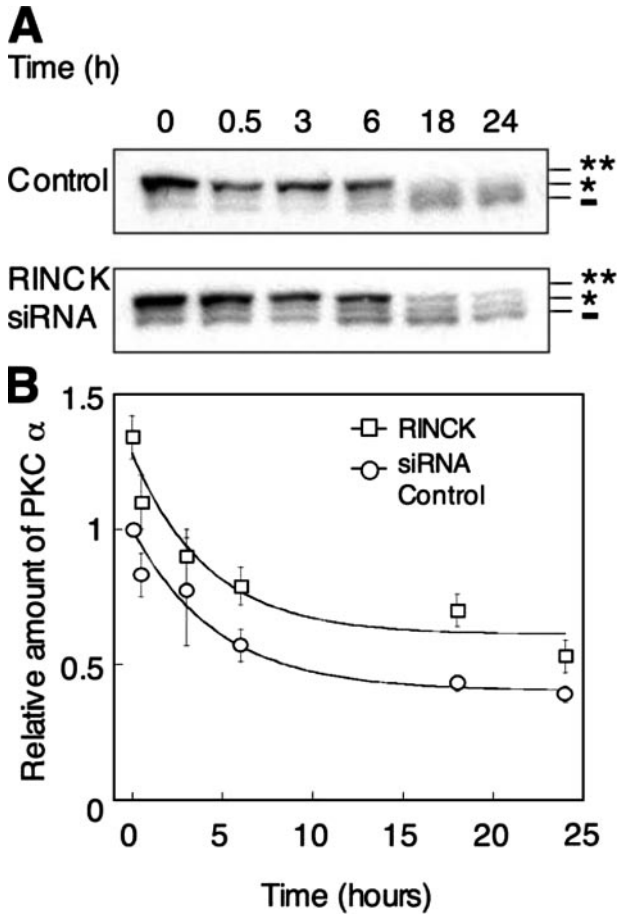

FIGURE 8. **The phorbol ester-mediated down-regulation of PKC is independent of RINCK.** Control nonspecific siRNA or RINCK siRNA were transfected into HeLa cells. Three days post-transfection, cells were treated with 200 nM PDBu for 0, 0.5, 3, 6, 18, and 24 h. *A*, Western blot showing the protein level of endogenous PKCα detected by an anti-PKCα antibody. *B*, quantification of the data in *panel A* showing the relative amount of PKCα in cells with control siRNA (*square*) or with RINCK siRNA (*circle*) at each time point. Data represent results from three independent experiments.

DISCUSSION

The cellular levels of PKC critically control the amplitude of signaling by this kinase and perturbations in the amount of PKC result in pathophysiological states. For example, PKCβII is grossly elevated in colon cancer, directly resulting in increased signaling that promotes colon carcinogenesis (5, 34). Similarly, PKC α, β, and ϵ are increased, and PKCδ is decreased, in non-small cell lung cancer cells, contributing to the increased survival and chemotherapeutic resistance of these cells compared with normal lung epithelial cells (3). Although the mechanisms controlling the maturation of PKC have been well studied, mechanisms controlling the turnover and degradation of the enzyme are less well understood. Early reports suggested that PKC was turned over by calpain-mediated proteolysis (20, 35), but more recent reports suggest the protein is degraded following ubiquitination (17–19). Here we identify a novel ubiquitin E3 ligase, RINCK, that binds the C1 domain of PKC and causes the ubiquitination and degradation of the kinase. This degradation mechanism is independent of the phosphorylation or activation state of PKC, suggesting that it generally controls the levels of cellular PKC, thus setting the amplitude of the PKC signal.

RINCK (TRIM41), an E3 Ligase for Protein Kinase C—RINCK belongs to the family of TRIM proteins, whose signature is a RING finger, B-box, and coiled-coil region (27, 28, 36). Over 70 mammalian TRIM genes have been identified, sharing the conserved NH_2-terminal tripartite motif, but differing in their COOH-terminal modules. These proteins are involved in an abundance of varied functions, including cell proliferation, apoptosis, cell cycle regulation, and viral responses. The mechanisms of these effects are not well understood; however, a growing number of these proteins have been shown to be E3 ligases, suggesting that their major role may be ubiquitination and protein degradation (36). RINCK1, corresponding to TRIM41β in GenBank™, has been recently reported to be an alternatively spliced protein that localizes to speckles in the cytoplasm and nucleus (30). Here we show that the protein functions as a ubiquitin E3 ligase directed at PKC family members. We have identified two alternatively spliced forms of RINCK, RINCK1 and RINCK2, which differ in the carboxyl-terminal residues. Western blot analysis reveals that RINCK1 is the predominant species of RINCK in the mammalian cell lines tested, which included COS7, HeLa, and tsA201 cells. Subcellular fractionation studies indicate that RINCK partitions equally in the detergent-soluble membrane fraction and the detergent-insoluble pellet, with very little in the cytosolic fraction. This detergent-soluble localization could correspond to the "speckles" location based on inmunolocalization of TRIM41β (30). The location of RINCK is consistent with reports that PKC is shunted for degradation at membrane and detergent-insoluble fractions (2, 18).

Both RINCK1 and RINCK2 are E3 ligases directed at PKC isozymes, with ligase activity that depends on the RING finger domain: mutation of the first conserved Cys in the metal coordination motif of the RING finger abolishes E3 ligase activity of RINCK. Interestingly, deletion of the first 19 amino acids of RINCK abolishes its autoubiquitination activity without impairing substrate ubiquitination. RINCK does not mediate the ubiquitination of the related kinase PKA.

RINCK Binds the C1A Domain of PKCβII—Co-immunoprecipitation and knockdown studies indicate that RINCK binds and regulates the levels of conventional, novel, and atypical PKC isozymes. This result is consistent with the finding that RINCK binds the C1A domain of PKC, a module conserved in all PKC isozymes. This interaction appears to be specific for the C1A domains of PKC family members because RINCK did not bind β2-chimaerin, a C1 domain-containing protein outside the PKC family (37). These data suggest that RINCK, through recognition of the C1A domain of PKC, is a specific E3 ligase for PKC family members.

RINCK Controls the Stability of PKC—Overexpression of RINCK causes a robust increase in the amount of ubiquitinated PKC and an accompanying reduction in the level of total PKC protein. Conversely, overexpression of the catalytically inactive CA mutant reduces the basal ubiquitination of PKC and causes a significant increase in the amount of PKC protein in unstimulated cells. Thus, RINCK controls the level of PKC in the basal, unstimulated state. Consistent with this result, genetic deple-

tion of RINCK increases the levels of conventional, novel, and atypical PKC isozymes. The magnitude of the effect is, however, cell-type dependent, underscoring the complexity of inputs controlling the degradation of PKC. Most notably, knockdown of RINCK in the breast cancer cell line results in a 2-fold increase in PKCα and PKCζ levels, and knockdown in the non-small cell lung carcinoma has no significant effect. Interestingly, H157 cells have elevated levels of PKC (3), presenting the possibility that compensating mechanisms that bypass RINCK have been established during the transformation of this cell line. Our results reveal that RINCK is one of likely many mechanisms that control the degradation of the PKC family.

RINCK also controls the amount of PKC following stimulation. PKC levels are elevated in cells depleted of RINCK, yet the half-time for phorbol ester-mediated degradation is the same for PKC from unstimulated or phorbol ester-stimulated cells. These data reveal that 1) RINCK degrades both activated PKC and inactive PKC, and 2) the RINCK-mediated degradation is independent of the phorbol ester-triggered degradation. Consistent with RINCK degrading active and inactive PKC in cells, *in vitro* studies revealed that RINCK ubiquitinates PKC independently of its activation state or phosphorylation state. Thus, RINCK controls the overall stability of PKC, independent of stimulation. The recognition of PKC independently of its phosphorylation state is consistent with the binding determinants being in the C1A domain, distal from the kinase core where the phosphorylation sites are. Perhaps what is more critical in the regulation of the degradation of PKC by RINCK is its location: activated PKC localizes first to the membrane and then, following prolonged stimulation, it becomes dephosphorylated and associates with the detergent-insoluble fraction of cells. RINCK localizes to both locations.

Considerable evidence indicates that the phorbol ester-dependent down-regulation of PKC requires the intrinsic catalytic activity of the kinase: inhibitors of PKC activity prevent down-regulation and kinase-inactive constructs are not sensitive to phorbol ester-dependent down-regulation (2, 19, 38). Yet kinase-inactive constructs of PKC are rapidly degraded in cells. This finding suggests that there are at least two mechanisms that control the degradation of PKC: one that regulates the basal level of bulk PKC and one that regulates the level of activated PKC. RINCK ubiquitinates all species of PKC it encounters, revealing that it is responsible for controlling the bulk levels of PKC.

How the ubiquitination catalyzed by RINCK is regulated to set the precise level of PKC remains to be established. However, localization of PKC at the site where RINCK localizes is likely to be a primary determinant in allowing degradation by this pathway. Thus, newly synthesized PKC that is not competent to mature associates with the detergent-insoluble pellet where it binds RINCK and is degraded. Similarly, activated PKC that becomes dephosphorylated associates with the detergent-insoluble pellet where it binds RINCK and is degraded.

Summary—The foregoing data identify RINCK as an E3 ligase that controls the amplitude of PKC signaling by controlling the amount of PKC in the cell. Whether defects in RINCK drive the altered PKC levels in human disease remains to be explored. This work also shows that the RINCK-controlled degradation of PKC is independent of the phorbol ester-mediated down-regulation, suggesting that additional E3 ligases mediate the phorbol ester-mediated ubiquitination and degradation of PKC. Thus, RINCK provides amplitude control in the PKC pathway by a mechanism that requires neither the phosphorylation nor activation of PKC isozymes.

Acknowledgments—We thank Marcelo Kazanietz for the cDNA for β2-chimaerin and Dan Dries for kinetic analysis of the data in Fig. 8.

REFERENCES

1. Newton, A. C. (2001) *Chem. Rev.* **101,** 2353–2364
2. Parker, P. J., Bosca, L., Dekker, L., Goode, N. T., Hajibagheri, N., and Hansra, G. (1995) *Biochem. Soc. Trans.* **23,** 153–155
3. Clark, A. S., West, K. A., Blumberg, P. M., and Dennis, P. A. (2003) *Cancer Res.* **63,** 780–786
4. D'Costa, A. M., Robinson, J. K., Maududi, T., Chaturvedi, V., Nickoloff, B. J., and Denning, M. F. (2006) *Oncogene* **25,** 378–386
5. Gokmen-Polar, Y., Murray, N. R., Velasco, M. A., Gatalica, Z., and Fields, A. P. (2001) *Cancer Res.* **61,** 1375–1381
6. Pan, Q., Bao, L. W., Kleer, C. G., Sabel, M. S., Griffith, K. A., Teknos, T. N., and Merajver, S. D. (2005) *Cancer Res.* **65,** 8366–8371
7. Regala, R. P., Weems, C., Jamieson, L., Khoor, A., Edell, E. S., Lohse, C. M., and Fields, A. P. (2005) *Cancer Res.* **65,** 8905–8911
8. Lu, Z., Xu, S., Joazeiro, C., Cobb, M. H., and Hunter, T. (2002) *Mol. Cell* **9,** 945–956
9. Pickart, C. M. (2001) *Annu. Rev. Biochem.* **70,** 503–533
10. Pickart, C. M. (2004) *Cell* **116,** 181–190
11. Laney, J. D., and Hochstrasser, M. (1999) *Cell* **97,** 427–430
12. Balendran, A., Hare, G. R., Kieloch, A., Williams, M. R., and Alessi, D. R. (2000) *FEBS Lett.* **484,** 217–223
13. Hansra, G., Garcia-Paramio, P., Prevostel, C., Whelan, R. D., Bornancin, F., and Parker, P. J. (1999) *Biochem. J.* **342,** 337–344
14. Jaken, S., Tashjian, A. H., Jr., and Blumberg, P. M. (1981) *Cancer Res.* **41,** 2175–2181
15. Solanki, V., Slaga, T. J., Callaham, M., and Huberman, E. (1981) *Proc. Natl. Acad. Sci. U. S. A.* **78,** 1722–1725
16. Lee, H. W., Smith, L., Pettit, G. R., and Smith, J. B. (1997) *Mol. Pharmacol.* **51,** 439–447
17. Lee, H. W., Smith, L., Pettit, G. R., Vinitsky, A., and Smith, J. B. (1996) *J. Biol. Chem.* **271,** 20973–20976
18. Leontieva, O. V., and Black, J. D. (2004) *J. Biol. Chem.* **279,** 5788–5801
19. Lu, Z., Liu, D., Hornia, A., Devonish, W., Pagano, M., and Foster, D. A. (1998) *Mol. Cell. Biol.* **18,** 839–845
20. Junoy, B., Maccario, H., Mas, J. L., Enjalbert, A., and Drouva, S. V. (2002) *Endocrinology* **143,** 1386–1403
21. Orr, J. W., Keranen, L. M., and Newton, A. C. (1992) *J. Biol. Chem.* **267,** 15263–15266
22. Vojtek, A. B., and Hollenberg, S. M. (1995) *Methods Enzymol.* **255,** 331–342
23. Orr, J. W., and Newton, A. C. (1994) *J. Biol. Chem.* **269,** 27715–27718
24. Joazeiro, C. A., Wing, S. S., Huang, H., Leverson, J. D., Hunter, T., and Liu, Y. C. (1999) *Science* **286,** 309–312
25. Anan, T., Nagata, Y., Koga, H., Honda, Y., Yabuki, N., Miyamoto, C., Kuwano, A., Matsuda, I., Endo, F., Saya, H., and Nakao, M. (1998) *Genes Cells* **3,** 751–763
26. Swerdlow, P. S., Finley, D., and Varshavsky, A. (1986) *Anal. Biochem.* **156,** 147–153
27. Nisole, S., Stoye, J. P., and Saib, A. (2005) *Nat. Rev. Microbiol.* **3,** 799–808
28. Reymond, A., Meroni, G., Fantozzi, A., Merla, G., Cairo, S., Luzi, L., Riganelli, D., Zanaria, E., Messali, S., Cainarca, S., Guffanti, A., Minucci, S., Pelicci, P. G., and Ballabio, A. (2001) *EMBO J.* **20,** 2140–2151
29. Saurin, A. J., Borden, K. L., Boddy, M. N., and Freemont, P. S. (1996) *Trends Biochem. Sci.* **21,** 208–214

30. Tanaka, M., Fukuda, Y., Mashima, K., and Hanai, R. (2005) *Mol. Biol. Rep.* **32,** 87–93
31. Keranen, L. M., Dutil, E. M., and Newton, A. C. (1995) *Curr. Biol.* **5,** 1394–1403
32. Borden, K. L., and Freemont, P. S. (1996) *Curr. Opin. Struct. Biol.* **6,** 395–401
33. Newton, A. C. (2003) *Biochem. J.* **370,** 361–371
34. Zhang, J., Anastasiadis, P. Z., Liu, Y., Thompson, E. A., and Fields, A. P. (2004) *J. Biol. Chem.* **279,** 22118–22123
35. Adachi, Y., Maki, M., Ishii, K., Hatanaka, M., and Murachi, T. (1990) *Adv. Second Messenger Phosphoprotein Res.* **24,** 478–484
36. Meroni, G., and Diez-Roux, G. (2005) *Bioessays* **27,** 1147–1157
37. Kazanietz, M. G. (2002) *Mol. Pharmacol.* **61,** 759–767
38. Ohno, S., Konno, Y., Akita, Y., Yano, A., and Suzuki, K. (1990) *J. Biol. Chem.* **265,** 6296–6300